Development of a Foreign Object Detection and Analysis Method for Wireless Power Systems

Neil Kuyvenhoven, C. Dean, J. Melton, J. Schwannecke, A.E. Umenei
Fulton Innovation, Access Business Group, Amway
Ada, Michigan
neil.kuyvenhoven@fultoninnovation.com

***Abstrac*t— In recent years, increased wireless power transfer systems technology research has led to systems with higher efficiency and more applicability over varying distances. Safety concerns associated with the technology are still challenges of major concern to the technology's expansion and adoption. Selective and qualitative detection of foreign objects around the system (metallic or magnetic objects) is of key importance due to their ability to absorb energy from the wireless power supply field in the form of heat (parasitic heating) and possibly become a hazard. This paper presents the development and experimental validation of the Power Loss Detection method (PLD). The algorithm was developed using mathematical regression analyses on experimental data to co-relate parameters obtained from analytic approximations of power in the system. The method developed is demonstrated by test data to be an effective method for analyzing wireless power systems for foreign object differentiation and detection. This method overcomes the disadvantages of cost, thermal regulation, response time, and size that plague other foreign object detection and parasitic heating sensing techniques.**

Keywords- Wireless Power Consortium (WPC), Qi, inductive power transfer, parasitic heating, magnetic heating, EM heating

I. INTRODUCTION

Wireless Power Systems (WPS), such as but not limited to that which is described by the Wireless Power Consortium (WPC) in the Qi standard [1], use coupled electromagnetic (EM) fields from a primary subsystem to transfer power through a nonconductive medium. The field is captured in a secondary subsystem and converted to useable energy. However, if there exists a material that can absorb EM fields, or in the terminology of the Qi standard a non-approved device in the EM field, while an Qi-approved (secondary subsystem) device is capturing power from the primary, such so-called foreign objects absorb energy from the field as well. In some cases this results in unacceptable levels of parasitic or foreign object heating. Furthermore, because of this energy loss, the transmitter subsystem delivers more power than necessary to sustain the intended power transfer rate requested by the secondary device, thus compromising the overall system efficiency and possibly leading to system failure and or damage.

For systems classified by the Qi standard as low power devices transferring up to 5W, the ability to heat a foreign object exists [1] and can heat objects above acceptable ISO safety standard levels [2]. This concern increases in prominence not only as the applicability of wireless power increases, but also as the power levels used in WPS increase. Developing algorithms and methods to make such systems safe and allow for seamless future growth is an issue of intense research and importance to the technology. For example, low power devices that use batteries are of real concern when using a WPS due to the adverse relation between increased temperatures with battery safety and performance. Ultimately, adding this type of intelligence to WPS allows for the safe and optimal use of wireless power today and in the future.

This paper describes the development of a novel method that dynamically evaluates the power budget of a WPS in real time with reasonable accuracy so as to identify when an unintended foreign object is absorbing power from the WPS generated field. The method described ensures further confidence and freedom for designers and manufacturers of the technology to do so with reduced risk of thermal heating in unintended objects. It compares this method on the merits of accuracy, responsiveness, and cost to the alternatives.

II. METHODS OF MONITORING AND DETECTING FOREIGN OBJECT HEATING IN A WPS

Several methods already exist to control the heating of foreign objects and the intended objects in a wireless power system. The level to which the heating must be controlled depends on many factors including the location of the component and the construction and material of the component amongst others. To understand the extent of control needed to keep induced temperatures to an acceptable range it is important to understand the mechanisms by which heat is generated in a wireless power system.

A typical WPS transmitter subsystem (like the transmitter referred to as type "A1" in the Qi standard) consists of a coil of litz wire that is driven through a capacitor in series by a pair of MOSFETs in a half-bridge configuration. Each of these components (the coil, the capacitor, and the MOSFETs) have ohmic losses. Secondly, the MOSFETs have an additional loss that is associated with the transition through their linear region. Additional components such as the permanent magnet

and ferrite core associated with the coils have hysteretic and eddy current losses. All of these losses, together with any other losses from the control circuit, result in an increase in ambient temperature in and around the transmitter. These losses can in turn raise the temperature through conduction and convection of any device or parasitic object placed on the transmitter surface.

The losses in the receiver subsystem that contribute to heat also include the ohmic losses in the power conversion electronics and coil. There are other significant and unavoidable losses which are accounted for and termed friendly parasitic losses. For example, if the receiver subsystem is a mobile phone then eddy currents can be induced in the metal housing of a battery, PCB, EMC shield, or any other unavoidable conductive or magnetic object in the device.

This system temperature can be controlled in many ways. It can be monitored using thermocouples or other such temperature sensors, when temperature readings reach a specific threshold or safety limit the power transfer is terminated. This solution suffers from high complexity due to the need for many I/O channels into the controller and a complex sensor array construction. Furthermore, inaccurate sensing and slow response time in the transmitter subsystem to external foreign object heating may result in elevated temperature levels. Heat sinks can be used on the transmitter to pull excess heat from a parasitic or powered device, but this requires a low thermal resistance between the heat sink and the device. It will also likely be too massive for many consumer electronic applications. In addition, the metal heat sink itself acts as a parasitic object subject to eddy current heating in the magnetic field. The surface of the transmitter can also be actively cooled with fans, heat pipes, or other methods of actively removing excess heat, but these suffer from high cost and complexity.

The method proposed in this paper, Parasitic Loss Detection (PLD), overcomes the disadvantages of cost, thermal regulation, response time, and size by understanding the loss mechanisms in the transmitter and receiver subsystems. It also takes into consideration how much power is consumed by the intended receiver subsystem. The premise of the algorithm and subsequent method being that if the power lost in the transmitter and receiver subsystems, together with the power delivered to the end device are quantified, summed and compared to the input power to transmitter, then any discrepancy must be in the form of a parasitic loss and if detected should trigger a shut down of the magnetic field. This work shows a method for understanding the loss in each transmitter and receiver component.

III. Algorithm Development

The algorithm is intended to estimate each of the loss elements in a WPS as defined by the Qi standard. The goal of a PLD solution is to detect when a foreign object heats to an unacceptable level; therefore, tight accuracies in power detection (down to the milli-watt levels) are not necessary as some amount of error in accurate power loss is tolerable as long as the foreign objects are identified with the algorithm and its inherent approximations.

A. Transmitter Subsystem Magnetic Losses

The magnetic losses on the transmitter subsystem are considered independently of that on the receiver subsystem due to the fact that the receiver subsystem is highly variable (different charging devices with different components and charge requirements).Yet the algorithm which is executed in the transmitter must work for all qualified Qi based receivers that are placed on it for power transfer.

The total losses in the primary subsystem are grouped into electronic losses (circuit and circuit components) and magnetic losses (EM interaction). The magnetic losses are subdivided into three classical categories including: anomalous, hysteretic, and eddy currently losses. The solution considers each of these separately [3-5]. The anomalous losses are considered negligible due to the fact that the magnetic material used for shielding, or core material, is considered homogenous. Likewise the hysteretic losses are significantly low and hence negligible due to the very soft composite magnetic materials used in the transmitter subsystem which have high permeability and very low hysteresis loss. These approximations leave the eddy current losses which are represented using the classical Bertotti's formula for power loss:

$$P_{eddy} \approx \frac{\pi^2 B_p^2 d^2 f^2}{6\rho D} \tag{1}$$

Where P is power dissipation (W/kg), B_p is peak flux density (T), d is thickness of the sheet or diameter of the wire (m), f is frequency (Hz), ρ is resistivity (Ωm), and D is specific density of the material (kg/m^3). These variables are constants based on the material, except for B_p and f, thus (1) can be rewritten as,

$$P_{eddy} \approx C \cdot B_p^2 \cdot f^2 \tag{2}$$

where C is a constant that represents all the material specific constants identified in (1). Furthermore, given that the composite material used for shielding is of high saturation magnetization, the systems are designed to operate without saturation. Thus due to the high permeability, an approximate linearity in the non-saturated portion of their BH curve can be assumed; therefore, B_p is approximated to be proportional to current I, $\left(B_p \approx \frac{\mu N}{l} * I \right)$ where N is the number of coil turns, L is the magnetic path length, and I is the current through the coil. So, (2) becomes,

$$P_{eddy} \approx C' \cdot I_{TxCoil}^2 \cdot f^2 \quad (3)$$

where I_{TxCoil} is the current of the transmitter coil. Thus the total magnetic losses are approximated by (3). Furthermore, noting the form of (3), it is evident that the coefficient C' can be estimated using the power law, $P = I^2 \cdot R$, where R is the difference between bare and 'in stack' ESR if frequency is kept constant in the transmitter coil. The ESR measured must be measured in stack, meaning all of the magnetic material that is to be considered with the power estimation is included in its appropriate location. Comparing (3) with the power law shows that,

$$R \approx C' \cdot f^2 \quad (4)$$

solving for C' and measuring the difference between 'in stack' and bare ESR of the primary coil across a constant frequency gives the coefficient for this term of the algorithm. The data shown in Fig. 1 supports the above extrapolation and approximation by showing that the C' remains constant over frequency.

B. Transmitter Subsystem Electronic Losses

The remaining power losses on the primary side are analyzed as ohmic or electronic losses. A Qi-based WPS transfers communication signals across the power coils on top of the power transfer. To measure this communication signal, a Qi transmitter typically has the ability to measure the coil current and the current from the rail which feeds the totem pole drive of the coil. The PLD algorithm takes advantage of these existing measurements and uses them for power analysis. The difference between these two readings is important. The coil current is an AC signal which contains a phase relationship with the voltage on the coil, and this current

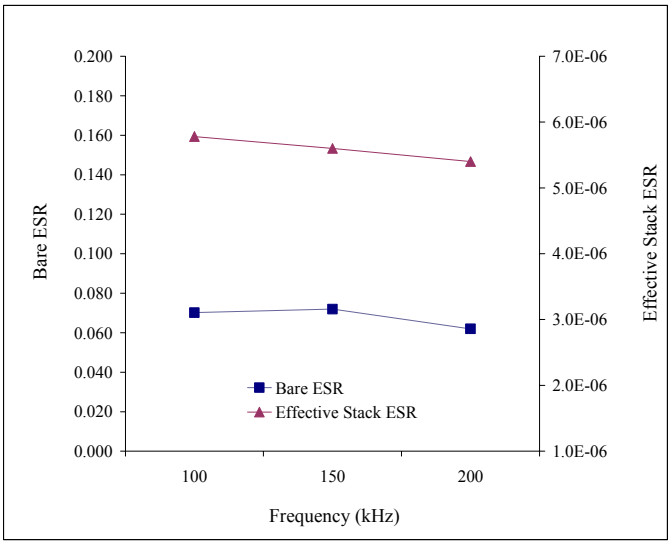

Figure 1. Equivalent series resistance over frequency

may be larger than the input current as the coil is part of a resonant tank. The coil current is a good measurement for power dissipated in the coil due to ohmic losses. The rail current, on the other hand, is theoretically a DC measurement and is a good measurement for power delivered to the coil. Practically, in a WPS, these current measurements will also have communication noise which must be filtered out in order to maintain accuracy in measurement.

The simplified calculation for the power lost in the coil looks similar to that of the eddy current loss. However, the ESR used for the coil current loss is the ESR of the bare coil. This is an important clarification because the bare ESR of the coil shows the true resistive loss that the coil contributes, whereas the ESR of the coil in stack shows the bare ESR losses in addition to the losses due to the magnetic material as it is measured 'in stack'. The coil current losses then follow the power law to take the form,

$$P_{TxCoil} \approx C \cdot I^2{}_{TxCoil} \quad (5)$$

where C effectively becomes the ESR of the bare transmitter coil which means it is independent of the presence of any magnetic material.

The losses in the primary electronics, excluding the coil, can be estimated as being proportional to rail current of the system. The amount of error introduced due to this assumption is insignificant as the power lost in the primary electronics aside from the power stage is relatively constant. With this understanding, the following form identifies the primary electronics losses,

$$P_{TxElec} \approx C \cdot I_{TxRail} \quad (6)$$

where I_{TxRail} is the current delivered from the voltage rail to the coil drive power stage in the transmitter.

Equations 3, 5 and 6 sum the losses in the transmitter to give the ideal form for the transmitter portion of algorithm as seen in (7).

$$P_{Tx} \approx C_0 \cdot \left(f \cdot I_{TxCoil}\right)^2 + C_1 + C_2 \cdot I_{TxRail} + C_3 \cdot I_{TxCoil}^2 \quad (7)$$

One could solve each of the coefficients of (7) individually and use superposition to combine the elements. However, using an experimentally gathered data set allows for a more accurate estimation of the system.

The simplicities in the formula when combined allows for polynomial-type relationships between the algorithm parameters. With this approach, and the fact that the formula references two different current measurements, I_{TxCoil} and I_{TxRail}, multivariate polynomial regression becomes a convenient method to obtain the solution. Experimental data was collected and used to obtain the parameters and coefficients in the algorithm form given in (7). Using

regression analysis with a typical P-value of 0.05, the ANOVA table was examined to determine the significance of the terms. The null hypothesis was rejected for rail current and the square of both rail current and the transmitter coil current making both statistically significant. This agreed with the form proposed in (7)

C. *Receiver Subsystem Losses*

The losses in the receiver subsystem were quantified and accounted for in a much simpler manner. The reason for this approach is due to the limited ability for the primary to gather real-time data from the receiver subsystem before control execution (due to the fact that this control method is to be executed from the transmitter subsystem). The proposed solution requires the secondary to provide its power loss nearly real-time as a single value. The coefficients also allow for a linear shift of the power reported from the receiver. This may be necessary for a number of reasons, one of them being the robustness of the solution when different transmitter and receiver subsystems may be used where the power reported must be altered. The result of the receiver subsystem coefficient is reported in the form,

$$P_{Rx} \approx C_4 \cdot P_{\mathrm{Re}c} + C_5 \tag{8}$$

where P_{Rec} is the power identified as loss in the receiver in the report obtained from the receiver. For the experimentally gathered data, the power loss in the secondary is measured via the difference in the RMS power received from the coil and the power delivered to the load as well as the ESR of the secondary coil multiplied by its current.

Combining (3), (7), and (8) gives the total analytic approximation used in the algorithm.

$$P_{input} \approx C_0 \cdot \left(f \cdot I_{TxCoil}\right)^2 + C_1 + C_2 \cdot I_{TxRail} + C_3 \cdot I_{TxCoil}^{\ 2} + C_4 \cdot P_{rec} + C_5 \tag{9}$$

The result shown in (9) accounts for all of the power in the system with the exception of the power due to the load on the receiver and that which is dissipated in a foreign object. The experimental setup measures the actual transmitter input power and output power to the load as well as all of the intermediate steps needed to complete the equation shown as (9). With this data the difference between the measured power loss in the system and the calculated power loss or expected power loss is identified as power loss in a foreign object which is in proximity of the field as shown in (10).

$$P_{measured} - P_{calculated} = P_{Foreign} \tag{10}$$

Since the algorithm is based on measurable or reported values to the transmitter, this equation can be calculated nearly real-time by the transmitter. The noted power loss is expected to be a foreign object absorbing magnetic field energy as produced by the transmitter. However, it is clear that a damaged component in the system such as a drive FET can also produce the same result. Therefore, the solution is true for an optimally functioning WPS.

It is also clear that the threshold of a failure must be large enough to allow for worse-case component and measurement tolerances. It has been demonstrated through empirical testing for WPC that 0.5W is the maximum allowable parasitic loss, for acceptable temperature rise.

IV. Test Setup and Results

The test setup involved a multi-channel, externally triggered, custom power analyzer that could separate communications from the power transfer. The transmitter was secured to an XY table while the receiver was secured to a fixture. This allowed the system to be tested at multiple positional offsets in the X and Z planes. It also made it possible to execute accurate and repeatable test setups as multiple passes were taken with different foreign objects and receivers. The power analyzer took multiple power measurements according to what was necessary for the algorithm. The power measurement locations are illustrated in fig. 2.

The measurements taken include power at each of the significant transitions. With these the power dissipated in each subsection of the device could be accurately calculated. All together a design of experiments was performed over fifteen foreign objects and four friendly parasitics at five positions

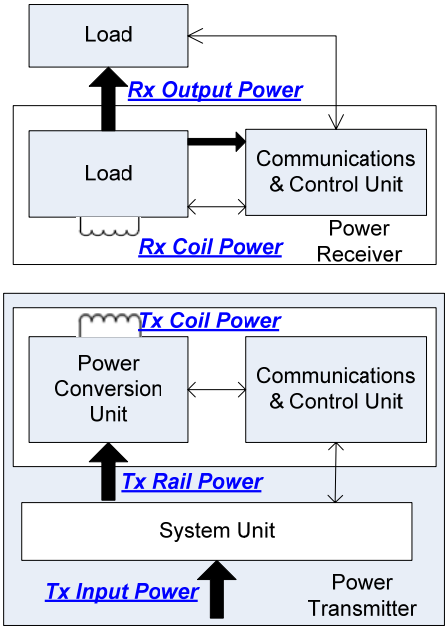

Figure 2. Measurement locations in the WPS

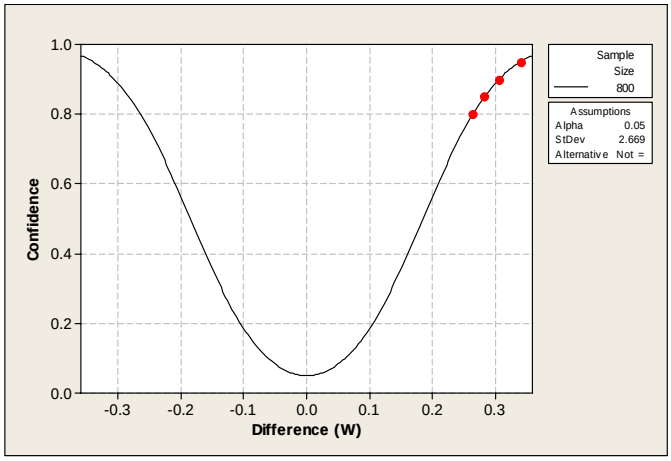

Figure 3. Confidence level for given power difference

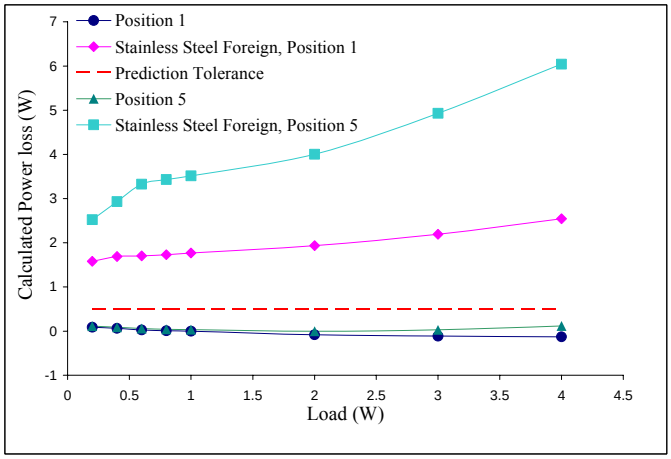

Figure 4. Algorithm result across load and position

and nine loads. The foreign objects included household items such as keys and coins as well as four 25mm defined metal discs. The foreign objects were chosen such that a range of materials covered paramagnetic, diamagnetic and worse case ferromagnetic materials. This gave a total of 3,200 individual test points with over 40 different measured variables at each point. Some of these variables were directly measured by the tester and other variables such as power on the transmitter coil were calculated by measuring the voltage and current.

To show that an adequate sample size was taken from the total population a 1-sample t-test was used, which gives confidence levels to show how far the sample input power mean differs from that of the population. Fig. 3 shows the curve of confidence levels at each corresponding difference associated with a sample size of 800 on which the aluminum friendly parasitic algorithm was based. Confidence levels of 0.80 to 0.95 are highlighted.

It can be shown that with the sample size of 800 data points the sample mean differs from the population mean by 0.34W with a confidence level of 0.95. This is the right most point on the graph above. The fact that the sample mean differs by less than the target of 0.5W shows that the sample is an adequate representation of the population. Using such a wide range of foreign objects and friendly parasitics gives the full variation of the population. Considering more data points would not be statistically beneficial to the accuracy of the algorithm.

Table 1 is a summary of the coefficients found using the methods described for receiver type A and transmitter type A1 as defined in the Qi standard with an aluminum shim behind the coil and shield assembly used to model the friendly parasitic elements found in a receiver subsystem (copper traces and battery). It should be noted that these coefficients are only suitable for the transmitter type A1. For different transmitter types the coefficients need to be re-evaluated.

TABLE I. COEFFICENTS FOR TYPE A1 TRANSMITTER

Coefficient	Value	Units
C0	0.00000439	Ohms/(kHz^2)
C1	0.342	Watts
C2	2.432	Volts
C3	0.0932	Ohms
C4	1.054	Unitless
C5	-0.000259	Watts

The algorithm was tested with the coefficients noted above and the system was tested with a set of foreign objects. The results showed a high level of success as seen in Fig. 4, where a subset of the experimental result is shown. The figure shows the data from testing the system at two positions with and without a foreign object between the transmitter and receiver.

Most notably the algorithm was able to distinguish between a large offset and the presence of a foreign object. The effect of the insertion of a foreign object is similar to a spatial offset between the transmitter and receiver in that the coupling factor between the transmitter and receiver coils is reduced. However, using frequency in the equation allows the primary to evaluate the power transfer and effective coupling factor at the expected frequency. Noting this difference, distinguishing between loss of coupling due to misalignment and foreign object becomes trivial.

V. CONCLUSION

The work presented herein shows the development and validity of a Power Loss Detection method to solve the need for foreign object detection in a WPS as defined by the Qi standard. This solution to foreign object detection maintains its effectiveness without having to wrap the technology with unnecessary additional safety mechanisms such as thermocouples and heatsinks. The Power Loss Detection method proposed allows for low cost implementation of the advanced algorithm and little to no additional hardware.

The algorithm in this work was demonstrated on the Qi low power standard. More experimental data is needed to prove its robustness before it is implemented in higher power systems. The need for this ability is apparent in low power wireless

transfer, and will be critical to higher power systems as small percentage losses in these systems can quickly become significant. The PLD solution discussed herein is a quick and easily implemented analytical algorithm that provides thermal differentiation at adequate safety levels for avoiding thermal problems and parasitic heating.

This work presents the results of a single transmitter type and a single receiver. Tests were performed at multiple relative positions and with different foreign objects inserted. Additional ongoing work includes: verification of the algorithm across multiple receivers to qualify that a single set of coefficients for a given transmitter with any receiver; a streamlined method of generating coefficients for specific transmitters so that the solution is viable; and development of a truncated test method for coefficient generation so suppliers of the technology can implement swiftly. The amount of testing required to understand the algorithm as was done for this effort is not necessary for new transmitter implementation as the procedure is developed and proven.

REFERENCES

[1] System description wireless power transfer Volume I: Low power, Part 1: Interface definition, Wireless Power Consortium v.1.0.1 Oct. 2010

[2] ISO 13732-1-2006, Ergonomics of the thermal environment – Methods for the assessment of human responses to contact with surfaces – Part 1: Hot surfaces, First Edition, Sept. 2006.

[3] G. Bertotti, Hysteresis in Magnetism, Acedemic Press, San Diego 1998.

[4] G. Bertotti, J. Magn. Magn. Mater. 112, 253 (1984).

[5] G. Bertotti, IEEE Trans. Magn. 24, 624 (1988).